Advances in Science and Technology Research Journal

Advances in Science and Technology Research Journal, 2025, 19(9), 105–116
https://doi.org/10.12913/22998624/206047
ISSN 2299-8624, License CC-BY 4.0

Received: 2025.05.05
Accepted: 2025.07.15
Published: 2025.08.01

CFD analysis of a wind panel with Savonius wind turbines

Przemysław Grzymisławski[1*], Dawid Półtoraczyk[1], Joanna Kałkowska[2]

[1] Institute of Thermal Energy, Poznan University of Technology, ul. Piotrowo 3, 60-965 Poznan, Poland
[2] Institute of Management and Information Systems, Poznan University of Technology, ul. Jacka Rychlewskiego 2, 60-965 Poznan, Poland
* Corresponding author's e-mail: przemyslaw.grzymislawski@put.poznan.pl

ABSTRACT

The paper presents the results of numerical analyses of a wind panel built of 6 vertical Savonious wind turbines. The basis for comparison were calculations made for a single turbine with the same parameters. Simulations were performed for six different directions of inflow, from almost parallel to the panel (5°) to almost perpendicular (85°). The calculations were performed using the Ansys FLUENT program, while the computational grids were prepared in the GMSH program. The aim of the analyses was to investigate the influence of the wind inflow angle on the panel on the amount of energy produced on subsequent turbines. The analysis covered the velocities between individual turbines and their influence on subsequent turbines. The calculations were performed as time-varying on a two-dimensional plane. Based on the obtained results, it was found that the inflow angle has a large influence on the efficiency of subsequent turbines as well as inflow velocity. For the angles up to 30° the aerodynamic wake behind subsequent turbines has a huge influence on the stability of the inflow on the next ones. For the cases from 45° the flow between turbines starts play significant role.

Keywords: wind energy, vertical axis wind turbines, CFD analysis, Savonius wind turbine, wind panel.

INTRUDUCTION

The diversity of wind conditions, i.e. wind energy potential, is not only regional (Coast, Wielkopolska, Mazovia, Suwałki Region), but also local, related to the local terrain and development of cities. The possibility of increasing the energy potential on a macro and micro scale can be used by using small or micro wind farms [1, 2]. The location of zones favorable for the development of wind energy is based not so much on the average annual wind speed, but on the analysis of the frequency of individual wind speeds in a given area (regional or local) [1]. This measured frequency of the limiting wind speed for the estimated profitability of wind farms (4 m/s) is a criterion for the implementation of a specific technical and organizational solution. The variability of the frequency of individual wind speeds is related not only to the seasons, but also to the intensity of solar radiation during the day. The shift in the daily peak time of electricity production and the increase in demand create a problem of energy storage or its resale to the external grid. In addition to these three issues, i.e. the location of zones favorable for wind speed, the frequency of its changes and the need for local storage and cooperation with an external network, the independence of wind turbine operation from the variability of the wind direction is also important. Most types of modern wind turbines operate regardless of the direction of the prevailing winds in Poland (westerly and south-easter). Information about this dominance allows for the optimization of the location of urban micro-wind turbines [3,4]. Wind conditions in cities are characterized by lower average speeds and greater turbulence due to the presence of buildings [5]. These factors can hinder the operation of turbines, which results in reduced efficiency [5, 6]. In such situations, it is not possible to use the standard assessment of resources that are developed for open areas. Adopting such

assumptions in urban conditions can lead to an overestimation of the turbine's efficiency [14, 5]. It is necessary to perform wind measurements at the planned turbine installation site [15, 16]. Despite these challenges, small wind turbines offer many advantages in urban environments. They can be integrated with existing infrastructure, require minimal transmission upgrades, and support local energy demand through net metering [17, 19]. Advances in turbine design, siting strategies, and control systems are being developed to better adapt to the turbulent and variable wind conditions typical of cities [17, 19]. In addition, the use of innovative materials and aerodynamic designs, such as vertical axis wind turbines (VAWTs), can increase efficiency and suitability for urban applications [20]. There are examples of innovative vertical axis wind turbine designs in the literature. One such design is the use of vanes to direct wind flow directly onto the turbine [21, 22]. Another example that uses a deflector directly onto the turbine is the use of a cylindrical deflector in front of side-by-side counter-rotating turbines [23]. Another example is the use of turbines with an overlapping work area [24], where the work of two, four and six turbines is combined. The disadvantage of the mentioned solutions is the need to set the turbine or a set of turbines in accordance with the wind direction.

Research is also being conducted for Savonius type turbines without the above-mentioned disadvantage. These are various types of ribs on the inner side of the blades [25], changing the shape of the blade [26, 27] or changing the size of the space between the blades (gap) [28].

In this article, the authors focused on the use of a panel consisting of a set of Savonius type turbines with a semicircular blade shape, without the use of guide vanes. The concept assumes the use of turbines positioned close to each other, but with the ability to operate regardless of the direction of the incoming wind. This type of solution is presented in [8,9], but it has not been described in the scientific literature.

MATERIALS AND METHODS

Geometrical model

A geometrical model of the turbine was prepared with dimensions given in Table 1. Figure 1 shows the geometry of a single turbine. Despite examples of using other blade shapes, as shown in [10, 11], the blades were made as semicircles. The domain for the panel was 66D length and 40D width. Distance between turbine axis was set to 1.974D (0.75 m), and there were six turbines in a row. The geometrical model of the domain was shown on Figure 3.

Table 1. Diameters of the turbine

Parameter	Symbol	Values [m]
Rotating domain radius	*Re*	0.30
Blade radius	*r*	0.10
Shift	*e*	0.02
Turbine diameter	*D*	0.38

Numerical model

Based on a geometry showed in Figure 1 a mesh for CFD calculation was prepared. Firstly a mesh for single turbine was prepared for calculate based values. After that a mesh for a whole panel was build. Mesh for a single turbine is shown in Figure 2 and it has 33880 elements. Domain for the single turbine has 70308 elements and for the wind panel – 378573 elements. For each case the mesh was build with 2D qaudrilateral elements. The grid parameter was shown in Table 2.

For both, single turbine and wind panel, turbine blades were modelled as zero-thickness wall. Calculations were performed as unsteady

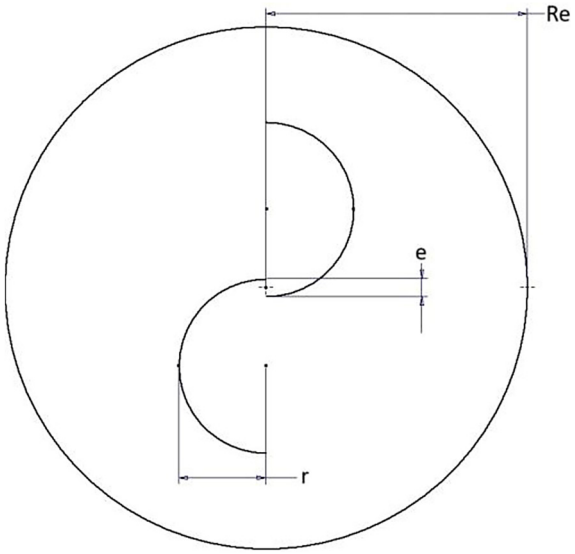

Figure 1. Dimension of the turbine and rotating domain

Table 2. Mesh parameters

Parameter	Minimum value	Maximum value
Orthogonal quality	0.345	0.999
Equiangle skew	<0.01	0.783
Y+	1	50
Aspect ratio	1.414	9.085

RANS with k-ω SST turbulence model and standard atmospheric conditions.

The rotating domain for turbines were set as mesh motion with axis of rotation individual for each turbine and rotational velocity equal 360°/s.

Authors in [12] performed calculation on 7 revolution and authors in [11] – 12.5. Based on that and controlling parameter during calculation a 9 rotation were selected. The inlet velocity was set to 5 m/s, 10 m/s and 15 m/s and the angles of inflow were changed for different cases. The angles were shown in Figure 3.

Time step was calculated as it was presented in [13]. Equation 1 describe the time for sliding mesh cases, and it should not be larger than time takes for a moving cell. In that case characteristic length L_c was equal 0.0004 m and velocity V was equal 0.596 m/s and it resulted time step Δt = 0.000223 s. Equation 2 takes number of blades as one of the parameter which gave time step Δt = 0.0318 s. For the presented calculation the time step was set to 0.0027777 s which correspond to 1° of rotation and 0.0013888 s which correspond to 0.5° of rotation. The calculations were considered to be convergent when a uniform torque curve was obtained for each turbine for 3 consecutive full revolutions. After convergence was achieved, calculations were made for the next three full turbine revolutions, which were subjected to final analysis. Simulation setup was presented in Table 3.

$$\Delta t = \frac{1 L_c}{3V} \tag{1}$$

$$\Delta t = \frac{1}{10} \frac{number\ of\ blades}{rotational\ velocity} \tag{2}$$

RESULTS

As the reference a maximum available energy from the wind was calculated based on Equation 3. By knowing the turbine diameter (0.38 m) and reference value for height in 2D calculations (1 m), the maximum available power was equal 29.09W, 232.75W and 785.53W according to 5 m/s, 10 m/s and 15 m/s respectively.

$$P_M = \frac{1}{2} \rho A V^3 \tag{3}$$

The numerical analysis in Ansys Fluent allows to control and save parameters of force and torque on the wall. For presented analysis a generated torque on each turbine was stored separately for each time step. By using equation 4 and 5 the instantaneous power were calculated. Following that a peak and mean power were calculated. From equation 6 power coefficient were calculated. The values for reference single turbine were presented in Table 4.

$$\omega = \frac{2\pi}{60} \cdot n \tag{4}$$

$$P_T = \mathrm{M} \cdot \omega \tag{5}$$

$$C_P = \frac{P_T}{P_M} \tag{6}$$

In the literature maximum power coefficient for vertical axis wind turbine based on numerical calculation for single, non-modified is equal:

Table 3. Simulation setup

Parameter	Type
Inlet	Velocity inlet; 5, 10, 15 m/s; magnitude and direction
Outlet	Pressure outlet
Turbulence	k-ω SST
Pressure-velocity coupling	SIMPLE
Turbine rotational speed	60 rpm
Timestep	0.0027777 s 0.0013888 s
Number of timesteps	Minimum 3960

– 5.3% [22],
– 3.8% [21],
– 23% [24],
– 23% [25],
– 24% [23].

The results obtained in the simulation are similar to the results obtained by other teams around the world.

Below a result from panels is presented. A peak and mean power are in Tables 5, 6, 7 and power coefficient in Tables 8, 9, 10. In all tables

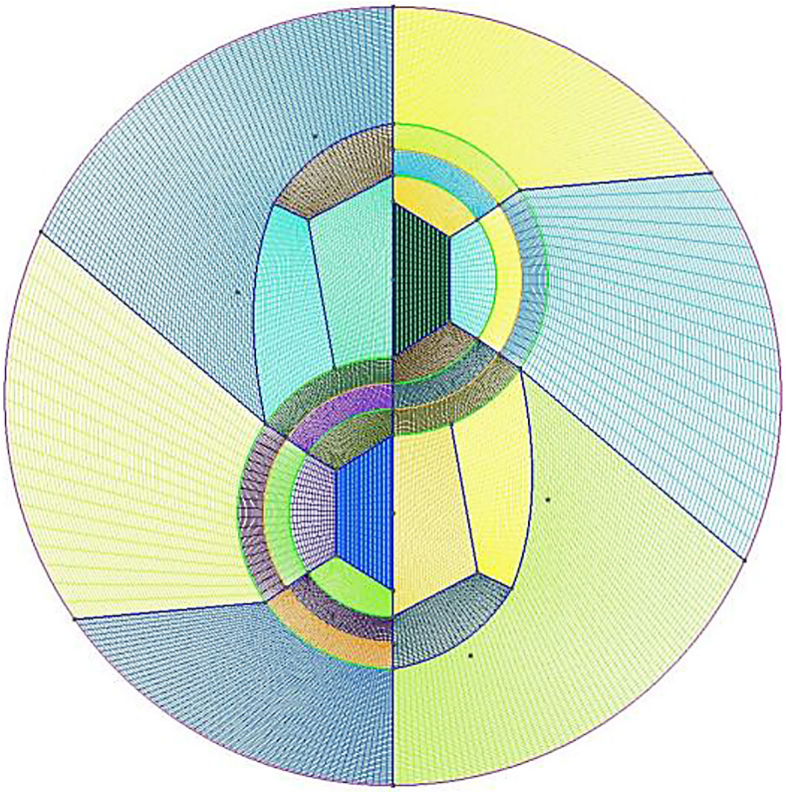

Figure 2. Mesh for a single turbine

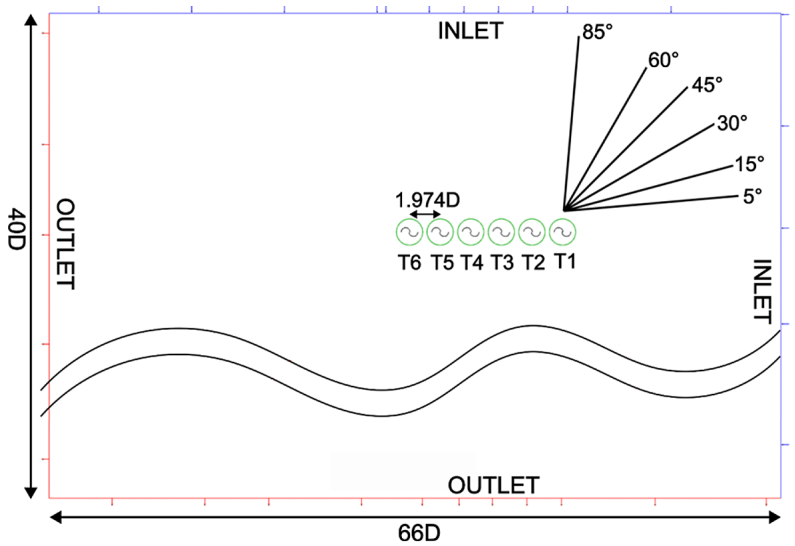

Figure 3. Whole domain with representation of inlet angles with focus on a turbines; outer blue line – inlet boundary condition, outer red line – outlet boundary condition, green circles – interfaces between rotating and stationary domains, black arcs – turbine blades

Table 4. Main parameters for reference single turbine

Parameter	Symbol	Values		
		5 [m/s]	10 [m/s]	15 [m/s]
Peak power	P_p	41.45 [W]	53.56 [W]	103.78 [W]
Mean power	P_m	6.14 [W]	25.66 [W]	5.51 [W]
Power coefficient	C_P	21.10 [%]	11.02 [%]	7.58 [%]

Table 5. Peak and mean power for each turbine – 5 m/s

Angle	5°		15°		30°		45°		60°		85°	
Turbine	Peak	Mean	Peak	Mean	Peak	Mean	Peak	Mean	Peak	Mean	Peak	Mean
T1	4.32	2.69	4.04	2.62	5.87	3.00	9.43	3.02	**23.39**	2.74	20.93	3.52
T2	7.49	2.33	4.98	2.37	7.29	2.51	7.82	2.98	19.47	3.09	18.23	3.52
T3	16.18	1.26	5.62	1.70	9.58	2.94	5.44	3.22	22.93	3.51	14.58	3.56
T4	**3.08**	0.87	6.13	1.22	8.57	3.06	5.44	3.12	20.07	3.53	13.97	3.64
T5	3.72	0.59	6.88	2.02	7.28	2.77	7.31	3.54	17.70	3.81	10.74	3.69
T6	4.46	**0.52**	4.95	1.67	7.98	2.73	8.47	3.47	10.89	4.65	18.91	**4.90**

Table 6. Peak and mean power for each turbine – 10 m/s

Angle	5°		15°		30°		45°		60°		85°	
Turbine	Peak	Mean	Peak	Mean	Peak	Mean	Peak	Mean	Peak	Mean	Peak	Mean
T1	22.79	10.37	22.22	11.26	25.73	12.04	31.79	12.15	27.20	10.50	33.95	12.59
T2	18.21	7.16	18.17	8.69	25.71	13.39	26.30	12.80	30.32	13.23	**39.10**	14.08
T3	13.27	4.10	25.78	8.98	26.86	13.23	27.95	14.16	29.77	13.32	36.76	13.76
T4	15.27	4.90	26.04	10.39	31.75	13.00	26.54	14.17	30.51	15.15	35.92	13.17
T5	12.99	4.43	31.29	10.57	31.45	14.93	30.18	15.42	31.28	15.17	35.32	13.65
T6	**8.47**	**3.78**	22.73	10.52	30.12	12.58	28.77	14.17	31.15	17.15	38.36	**18.27**

Table 7. Power coefficient for 15 m/s

Angle	5°		15°		30°		45°		60°		85°	
Turbine	Peak	Mean	Peak	Mean	Peak	Mean	Peak	Mean	Peak	Mean	Peak	Mean
T1	41.30	21.69	46.52	23.28	51.77	25.91	65.02	26.77	62.19	24.94	65.49	28.18
T2	**30.60**	**9.01**	55.78	20.74	61.47	27.61	72.33	29.38	70.10	32.62	**85.25**	30.91
T3	47.61	13.86	57.36	23.70	61.73	28.82	74.61	30.39	68.77	30.55	86.42	31.65
T4	53.95	14.47	61.27	21.95	70.83	27.88	63.33	32.14	72.66	36.29	85.05	32.48
T5	41.21	11.78	57.19	22.57	71.38	30.42	72.90	33.40	74.73	37.24	79.35	33.82
T6	59.94	14.20	60.44	23.90	64.89	25.89	69.90	28.95	83.77	38.90	74.66	**38.94**

maximum and minimum values were marked with, accordingly, green and red colour. It can be noticed, that values in wind panel are lower than a single turbine. It is caused by the direct wake from preceding turbines, for low inflow angles, and to a lesser extent from turbulence between turbines for high inflow angles.

Comparing all above data it can be seen, that for higher inflow velocity, the overall efficiency of the turbine drop down. The highest values of power coefficient are for inflow angles higher than 60°. It causes by more uniform flow for each turbine – turbines aren't in the wake of the previous turbine. The wake for inflow angle equal 5° was shown on Figure 4. Figure 5 present more uniform velocity profile between turbines for inflow angle equal 60° and on Figure 6 there is configuration 85° and 5 m/s.

Table 8. Power coefficient for 5 m/s

Turbine	Angle					
	5°	15°	30°	45°	60°	85°
T1	9.25%	9.01%	10.31%	10.38%	9.42%	12.10%
T2	8.01%	8.15%	8.63%	10.24%	10.62%	12.10%
T3	4.33%	5.84%	10.11%	11.07%	12.06%	12.24%
T4	2.99%	4.19%	10.52%	10.72%	12.13%	12.51%
T5	2.03%	6.94%	9.52%	12.17%	13.10%	12.68%
T6	**1.79%**	5.74%	9.38%	11.93%	15.98%	**16.84%**

Table 9. Power coefficient for 10 m/s

Turbine	Angle					
	5°	15°	30°	45°	60°	85°
T1	4.46%	4.84%	5.17%	5.22%	4.51%	5.41%
T2	3.08%	3.73%	5.75%	5.50%	5.68%	6.05%
T3	1.76%	3.86%	5.68%	6.08%	5.72%	5.91%
T4	2.11%	4.46%	5.59%	6.09%	6.51%	5.66%
T5	1.90%	4.54%	6.41%	6.63%	6.52%	5.86%
T6	**1.62%**	4.52%	5.40%	6.09%	7.37%	**7.85%**

Table 10. Power coefficient for 15 m/s

Turbine	Angle					
	5°	15°	30°	45°	60°	85°
T1	2.76%	2.96%	3.30%	3.41%	3.17%	3.59%
T2	**1.15%**	2.64%	3.51%	3.74%	4.15%	3.93%
T3	1.76%	3.02%	3.67%	3.87%	3.89%	4.03%
T4	1.84%	2.79%	3.55%	4.09%	4.62%	4.13%
T5	1.50%	2.87%	3.87%	4.25%	4.74%	4.31%
T6	1.81%	3.04%	3.30%	3.69%	4.95%	**4.96%**

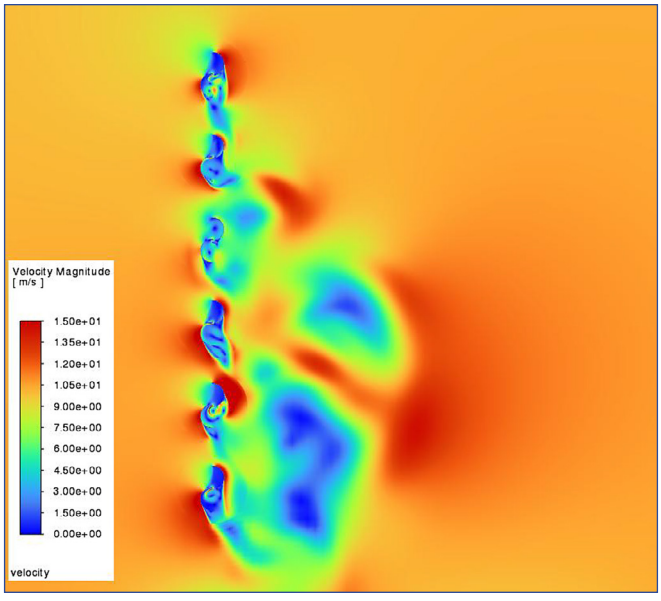

Figure 4. Velocity profile for inflow angle equal 5° and inlet velocity equal 10 m/s

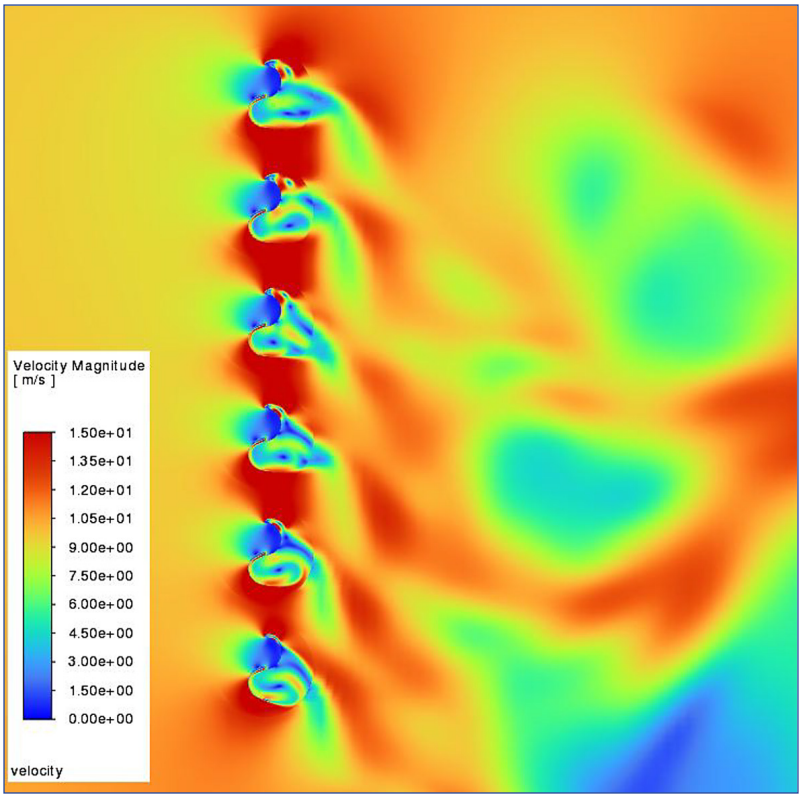

Figure 5. Velocity profile for inflow angle equal 60° and inlet velocity equal 10 m/s

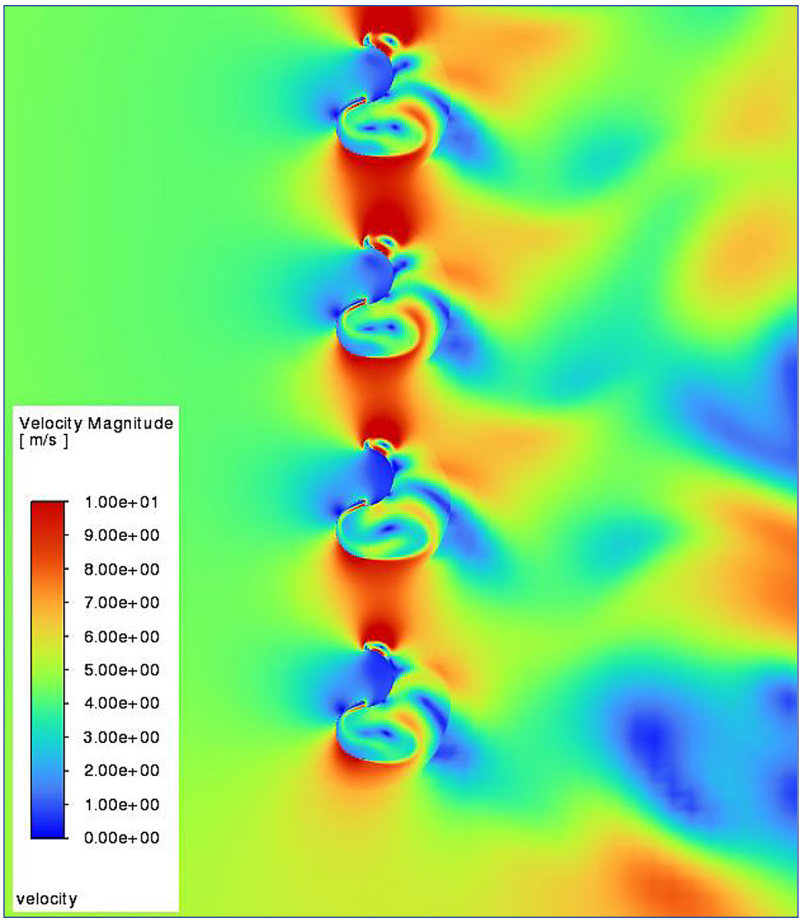

Figure 6. Velocity profile for inflow angle equal 85° and inlet velocity equal 5 m/s

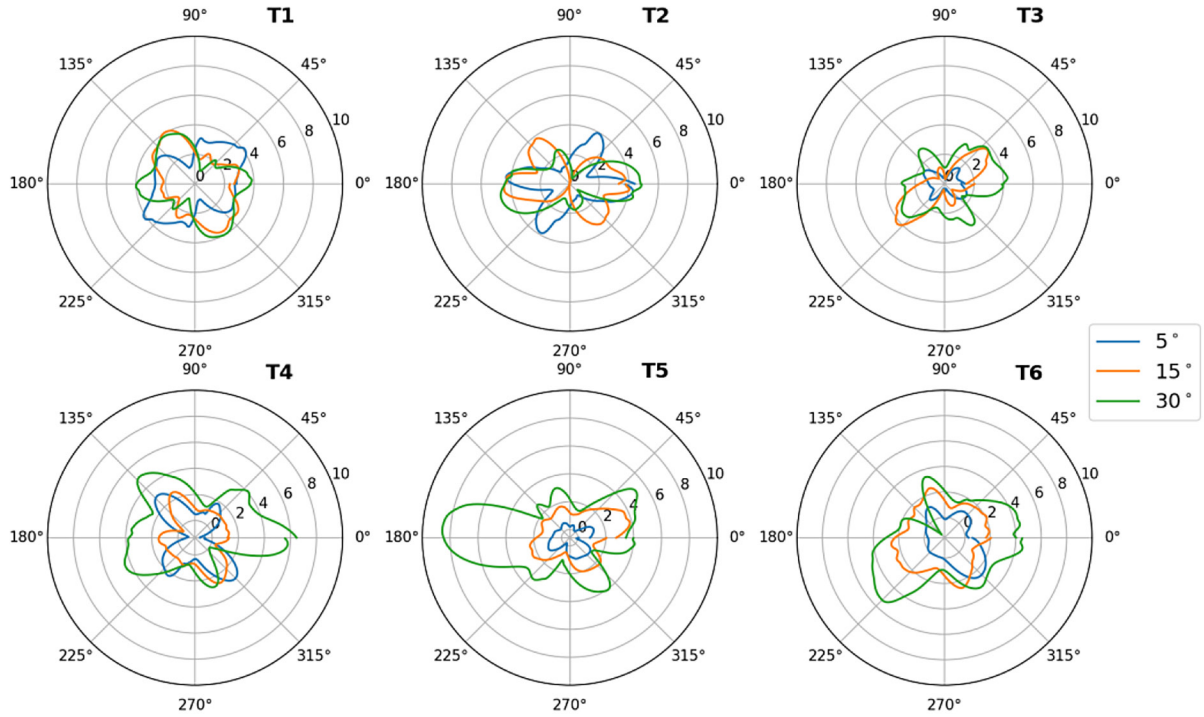

Figure 7. Power output from turbines at 5°, 15° and 30° inflow, 5m/s

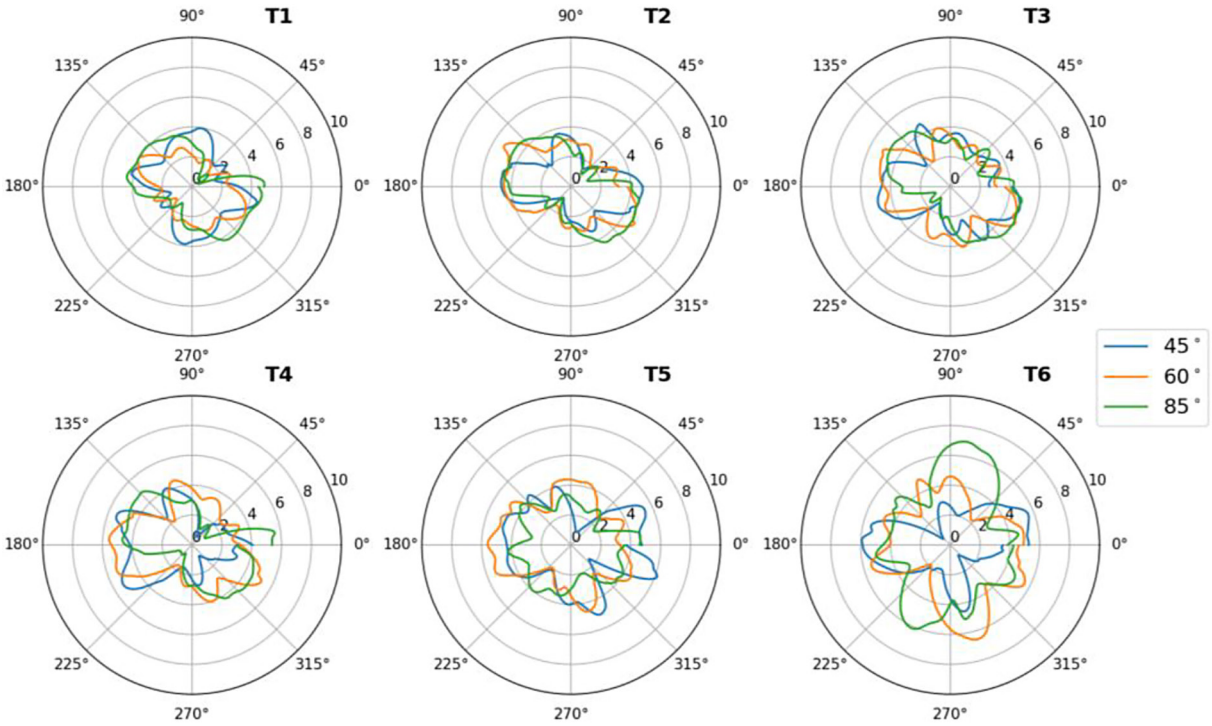

Figure 8. Power output from turbines at 45°, 60° and 85° inflow, 5m/s

For almost perpendicular inflow on the panel the power coefficient isn't uniform. The highest value is for the last turbine in the row which is caused by the interference between turbines. It is well seen on Figure 6, where velocity profile between turbines T6 and T5 (first and second from the bottom) characterised lower values than for upper turbines – T5 and T4, T4 and T3. It correspond to the higher value of negative force on the outter side of blades.

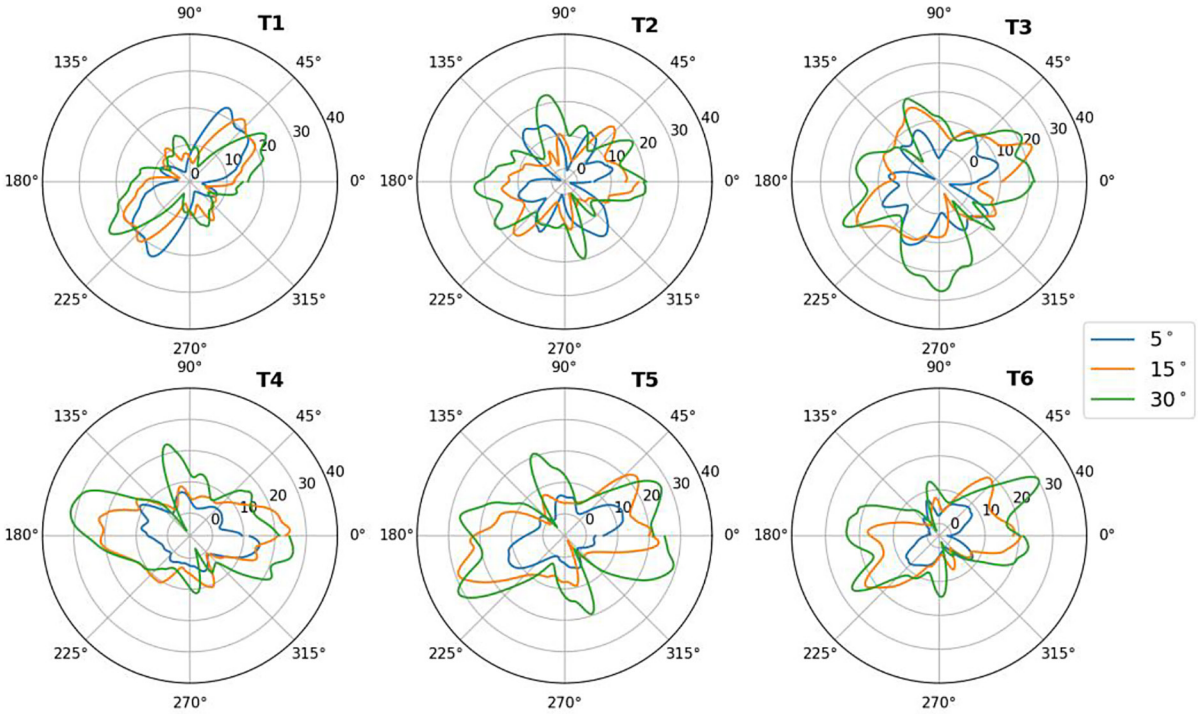

Figure 9. Power output from turbines at 5°, 15° and 30° inflow, 10m/s

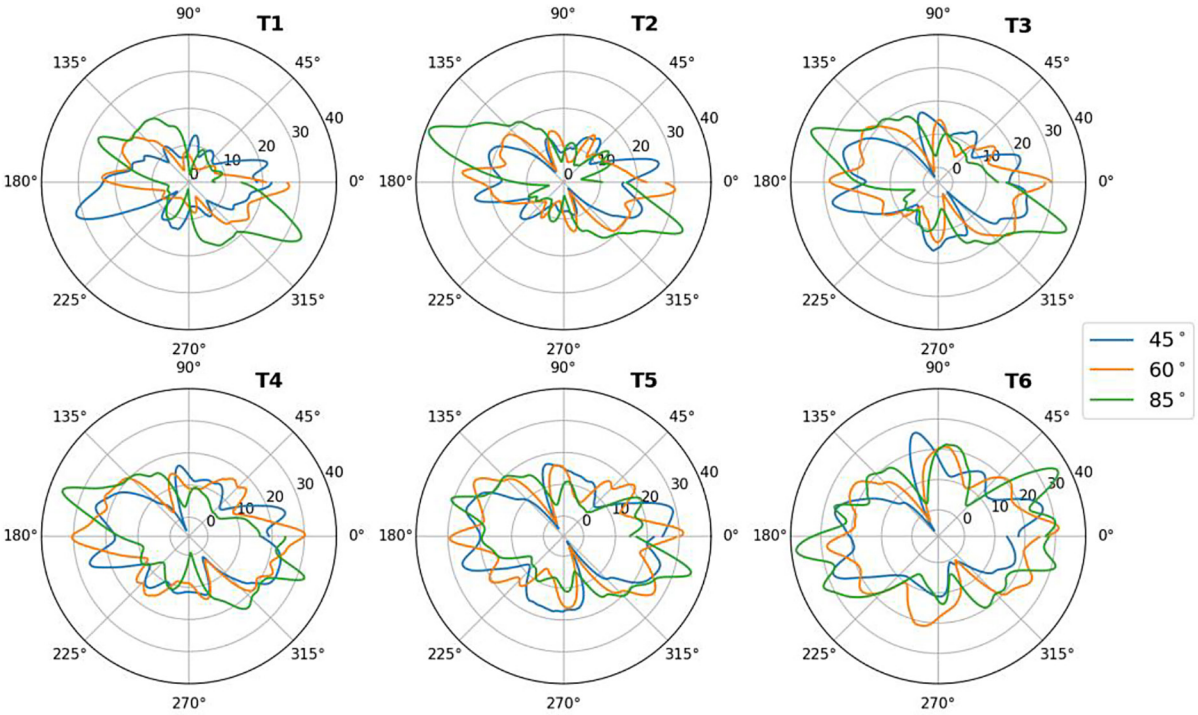

Figure 10. Power output from turbines at 45°, 60° and 85° inflow, 10m/s

The Figures 7–12 shows non uniform power distribution for the turbines in wind panel. For low inflow angles it is very chaotic for last turbines in the panel. The last turbine is in a very strong aerodynamic wake caused by the previous turbines and the local inlet velocity is lower than for the turbine T1. The most stable condition – the most symmetric power output – can be obtained on Figure 9 for T1. In general, T1 characterise the most predictable power output for each case.

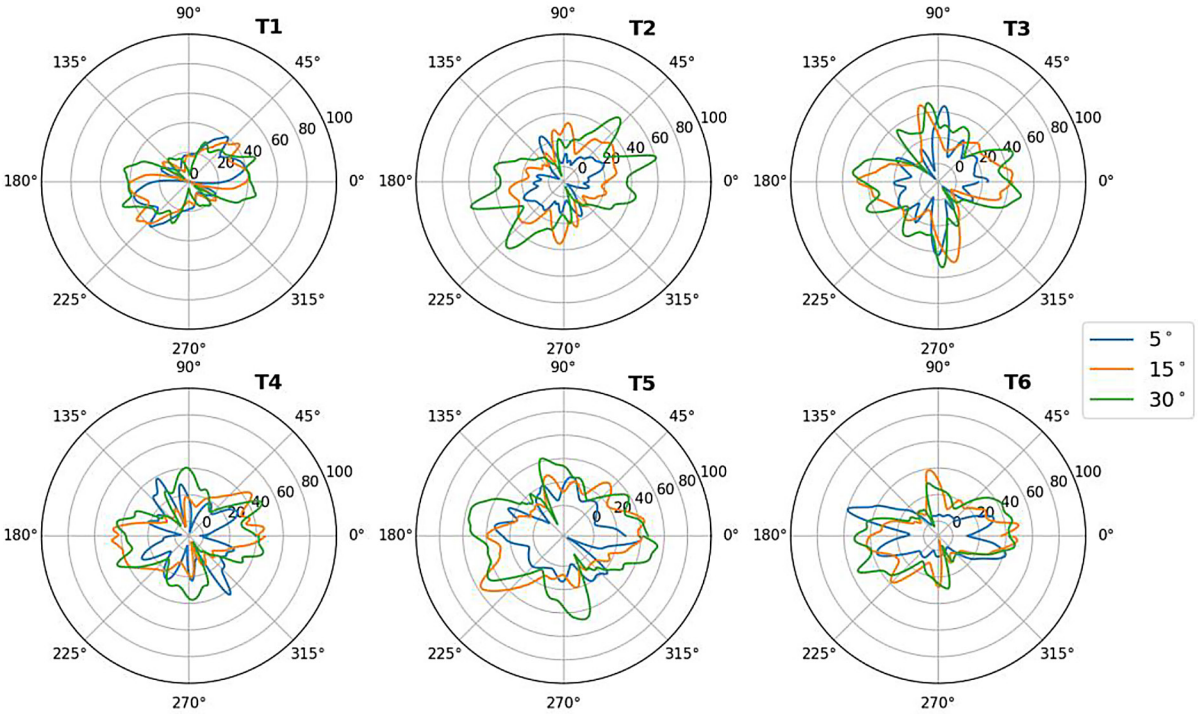

Figure 11. Power output from turbines at 5°, 15° and 30° inflow, 15m/s

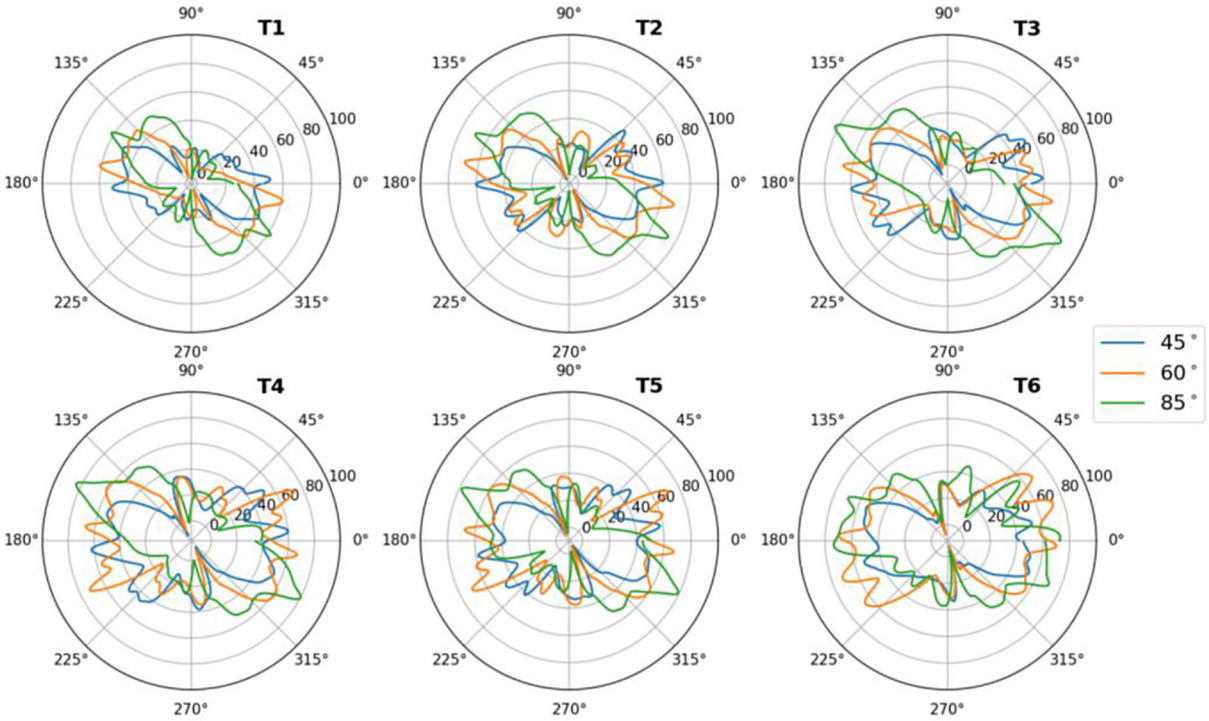

Figure 12. Power output from turbines at 45°, 60° and 85° inflow, 15m/s

CONCLUSIONS

Analysing the presented results, one can conclude that the flow between them has a very large impact on the amount of energy produced by individual turbines. For the cases with an inflow angle of 5°, the amount of energy produced along the panel decreases, however, looking at the other cases, we do not have such a sudden drop in efficiency on the subsequent turbines. It is also worth

noting that the first turbine in the row does not generate the highest power in the entire panel. In the case of an inflow angle of 85°, which is the closest to the perpendicular, one could expect uniform operation of all turbines, significant differences between the amount of energy produced by them can be seen. The inflow velocity plays important role to power coefficient, but not for the overall phenomena of power coefficient distribution between inflow angles.

It should also be taken into account that the calculations were prepared and performed in two-dimensional space. This may also be important in the context of the flowing fluid, especially if we accept for analysis the case in which a single turbine was presented with undisturbed flow around it. Analysing the average power generated by the turbine in the case of an inflow angle of 85°, the highest mean power was obtained by turbine number 6 for all velocity cases.

The presented results show that the amount of generated energy with the increase of the inflow angle will change in favour of the one closer to the perpendicular, however, the amount of energy produced individually by each turbine will not be the same as in the case of a single turbine positioned far from obstacles.

The most important thing for authors in the future work is to known the phenomena of turbulence between turbines. Other distance between turbines and different rotation direction will be taken into account. The conversion from 2D to fully three-dimensional with greater mesh density and change the turbulence model and calculation method to LES or DES in order to increase the accuracy of the obtained results. It will also be important to conduct an experiment in a wind tunnel for the presented turbines with the possibility of changing the angle and inflow velocity settings. It will allow to compare simulation results with experimental results.

REFERENCES

1. Cichoń, A.; Malinowski, P.; Mazurek, W., Porównanie możliwości wykorzystania małych turbin wiatrowych o poziomej i pionowej osi obrotu, Przegląd Elektrotechniczny, 2016/09, 92, https://doi.org/10.15199/48.2016.09.63
2. Poplawski, T., Problematyka prognoz generacji wiatrowej w KSE, Przegląd Elektrotechniczny, 2014; 7(90): 119–122, https://doi.org/10.12915/pe.2014.07.23
3. Boczar, T.; Szczyrba, T., Ocena wpływu warunków meteorologicznych na sprawność turbin wiatrowych, Pomiary, Automatyka, Kontrola, 2012; 58(12), 1044–1047.
4. Jarzyna, W.; Pawłowski, A.; Viktorich, N., Technological development of wind energy and compliance with requirements for sustainable development, Problems of Sustainable Development, 2014; 9(1): 167–177.
5. Anup, K.C.; Whale, J.; Urmee, T., Urban wind conditions and small wind turbines in the built environment: A review;, Renewable Energy, 2019; 131: 268–286. https://doi.org/10.1016/j.renene.2018.07.050
6. Pagnini, L.C.; Burlando, M; Repetto, M.P., Experiment power curve of small size wind turbines in turbulent urban environment, Applied Energy, 2015; 154: 112–121. https://doi.org/10.1016/j.apenergy.2015.04.117
7. Firdaus, B.; Izwan, I.; Thamir, K. I.; Daing, M. N. D. I.; Shahrani, A., A study on the power generation potential of mini wind turbine in east coast of Peninsular Malaysia, AIP Conference Proceedings, 2017, 1826, https://doi.org/10.1063/1.4979239
8. VINDPANEL. Available online: https://www.vindpanel.com/ (accessed on 17-04-2025).
9. New Atlas. Available online: https://newatlas.com/energy/wind-turbine-wall-doucet/ (accessed on 15-04-2025).
10. Zemamou, M.; Aggour, M.; Toumi, A., Review of Savonius wind turbine design and performance, Energy Procedia, 2017; 141: 383–388, https://doi.org/10.1016/j.egypro.2017.11.047
11. Im, H.; Kim, B. Power, performance analysis based on savonius wind turbine blade design and layout optimization through rotor wake flow analysis, Energies, 2022; 15: 9500, https://doi.org/10.3390/en15249500
12. Mohamed, M.; Dessoky, A.; Hafiz, A. A., CFD analysis for H-rotor Darrieus turbine as a low speed wind energy converter, Engineering Science and Technology, an International Journal, 2014; 9(18). https://doi.org/10.1016/j.jestch.2014.08.002
13. Alaimo, A.; Esposito, A.; Messineo, A.; Orlando, C.; Tumino, D, 3D CFD analysis of a vertical axis wind turbine, Energies, 2015; 4: 3010–3033. https://doi.org/10.3390/en8043013
14. Acosta, J.L.; Combe, K.; Djokic, S.Z.; Hernando-Gil, I., Performance Assessment of Micro and Small-Scale Wind Turbines in Urban Areas, IEEE Systems Journal, March 2012; 6(1). https://doi.org/10.1109/JSYST.2011.2163025
15. Zagubien, A.; Wolniewicz, K., Energy efficiency of small wind turbines in an urbanized area – case studies, Energies 2022; 15(14). https://doi.org/10.3390/en15145287

16. Firoz, A.; Yingai, J., The Utilisation of Small Wind Turbines in Built-Up Areas: Prospects and Challenges, Wind 2023; 3(4): 418-138. https://doi.org/10.3390/wind3040024
17. Ferrigno, Kevin J., Challenges and strategies for increasing adoption of small wind turbines in urban areas (2010).
18. Amer, A.; Azab, A.; Maher, A.A.; Awad, A.S.A., A stochastic program for siting and sizing fast charging stations and small wind turbines in urban areas, IEEE Transactions on Sustainable Energy, April 2021; 12(2). https://doi.org/10.1109/TSTE.2020.3039910
19. Battisti, L.; Benini, E.; Brighenti, A.; Dell'Anna, S.; Raciti Castelli, M., Small wind turbines effectiveness in the urban environment, Renewable Energy, 2018; 129(Part A), 102–113. https://doi.org/10.1016/j.renene.2018.05.062
20. Appadurai, M.; Fantin Irudaya Raj, E.; Lurthu Pushparaj, T., Sisal fiber-reinforced polymer composite-based small horizontal axis wind turbine suited for urban applications – a numerical study, Emergent Materials 2022; 5: 565–578. https://doi.org/10.1007/s42247-022-00375-x
21. Ghafoorian, F.; Mirmotahari, S.R.; Mehrpooya, M.; Akhlagi, M., Aerodynamic performance and efficiency enhancement of a Savonius vertical axis wind turbine with Semi-Directional Curved Guide Vane, using CFD and optimization method, Journal of the Brazilian Society of Mechanical Sciences and Engineering 2024; 46: 443. https://doi.org/10.1007/s40430-024-05030-6
22. Ghafoorian, F.; Mirmotahari, S.R.; Wan, H., Numerical study on aerodynamic performance improvement and efficiency enhancement of the Savonius vertical axis wind turbine with semi-directional airfoil guide vane, Ocean Engineering, 2024; 307.
23. Fatahian H.; Mishra R.; Jackson F.F.; Fatahian E., Design optimization of an innovative deflector with bleed jets to enhance the performance of dual Savonius turbines using CFD-Taguchi method, Energy Conversion and Management, 2023; 296.
24. Wenlong Tian; Xiwen Ni; Zhaoyong Mao; Yan-Feng Wang, Study on the performance of a new VAWT with overlapped side-by-side Savonius rotors, Energy Conversion and Management, 2022; 264.
25. Al-Gburi, K.A.H.; Alnaimi, F.B.I.; Al-quraishi, B.A.J.; Tan, E.S.; Kareem, A.K. Enhancing Savonius vertical axis wind turbine performance: a comprehensive approach with numerical analysis and experimental investigations. Energies 2023; 16: 4204. https://doi.org/10.3390/en16104204
26. Zemamoua, M., Aggoura, M., Toumi, A. Review of Savonius wind turbine design and performance, Energy Procedia, 2017; 141: 383–388, https://doi.org/10.1016/j.egypro.2017.11.047
27. Heejeon I.; Bumsuk K. Power performance analysis based on Savonius wind turbine blade design and layout optimization through rotor wake flow analysis, Energies 2022; 15: 9500. https://doi.org/10.3390/en15249500
28. Swidyrczuk, J.; Doerffer, P.; Szymaniak, M. Unsteady flow through the gap of Savonius turbine rotor, Task Quartelry 2011; 15(1): 59–70.